

Solving the Residual Lithium Problem by Substoichiometric Synthesis of Layered Ni-Rich Oxide Cathodes

Leonhard Karger,^a Rui Yao,^a Karsten Seidel,^b Barbara Nascimento Nunes,^a Ananyo Roy,^a Ruizhuo Zhang,^a Jürgen Janek,^{a,c} Aleksandr Kondrakov,^{a,b*} and Torsten Brezesinski^{a*}

^a Battery and Electrochemistry Laboratory (BELLA), Institute of Nanotechnology, Karlsruhe Institute of Technology (KIT), Kaiserstr. 12, 76131 Karlsruhe, Germany.

^b BASF SE, Carl-Bosch-Str. 38, 67056 Ludwigshafen, Germany.

^c Institute of Physical Chemistry & Center for Materials Research (ZfM/LaMa), Justus-Liebig-University Giessen, Heinrich-Buff-Ring 17, 35392 Giessen, Germany.

*Email: aleksandr.kondrakov@basf.com, torsten.brezesinski@kit.edu

Abstract

Herein, we deliberately used substoichiometric amounts of lithium hydroxide for preparing layered Ni-rich oxide cathode materials, with minor or even no residual lithium being present on the particle surface. This approach allows achieving record capacities with LiNiO_2 while using up to 7% less lithium and avoiding tedious post-processing steps, thus facilitating synthesis and improving battery performance.

Layered Ni-rich oxide cathode active materials (CAMs) offer a combination of unique properties for application in lithium-ion batteries (LIBs), but usually contain residual lithium on the particle surface as a result of their synthesis history.^[1] For LiNiO_2 (LNO), the semi-structural formula $(\text{Li}_x\text{Ni}_{1-x})\text{NiO}_2$ can be used to understand effects arising from the lithium-to-nickel ratio since at close-to-stoichiometric conditions only intrinsically present $\text{Ni}_{\text{Li}}^{\bullet}$ and no $\text{Li}_{\text{Ni}}^{\bullet\bullet}$ point defects (as can be assumed from the notion of cation mixing) exist.^[2] The effect of the latter ratio on CAM quality has been studied, and a positive effect of using lithium excess in the synthesis has been identified, due to formation of fewer $\text{Ni}_{\text{Li}}^{\bullet}$ defects,^[3,4] which are associated with kinetic hindrance near the end of discharge.^[1,5,6] However, when considering the intrinsically defective nature of LNO, excess lithium from overstoichiometric concentrations is deposited onto the particle surface in the form of carbonates, hydroxides, and/or oxides.^[7-9] This necessitates the application of post-treatment steps such as washing, which may negatively affect the material and further lead to additional processing time and wastewater generation,^[10,11] and therefore to higher costs and more severe environmental impact.

Herein, we tackle this problem by first acknowledging the need of using less lithium than required for preparing stoichiometric LNO. Secondly, uniform lithium distribution

needs to be ensured to produce high-quality CAMs at substoichiometric lithium-to-nickel ratios. Overall, we believe that our study helps clear a major hurdle towards widespread application of Ni-rich cathodes by avoiding the necessity of water washing and the subsequent structural damage to the particle surface (H^+/Li^+ exchange, rock salt formation during post-annealing, etc.), ultimately achieving better synthesis results under more cost-effective and environmentally sustainable conditions.

State-of-the-art (SoA) synthesis of LNO makes use of lithium excess to ensure good material quality. However, the residual lithium needs to be removed in a series of steps, also requiring post-annealing, as schematically illustrated in **Figure 1**.^[1,12,13] Conversely, our approach only involves an intermediate mixing step, which adds to processing complexity but also offers the possibility of tailoring the calcination process, due to higher throughput from increased oven loadings. This is because of the precursor dehydration in the initial pre-calcination step.^[14] As a prototype material, LNO was chosen and prepared using the residual-free (RF) method described herein. Specifically, we examined a range of lithium-to-nickel ratios, with pre-calcination performed at 300 °C under inert (RF-Ar- y) and oxidizing conditions (RF-O₂- y). Of note, y in the acronyms refers to the ratio of lithium to nickel in the actual synthesis. The same nomenclature is also applied to the reference SoA samples. XRD revealed the presence of NiO and Li₂O after this initial heating step, indicating successful removal of water (**Figure S1**, Supporting Information). Finally, the precursor blends were calcined at 700 °C under oxygen flow.

State-of-the-art Procedure



Residual-free Method

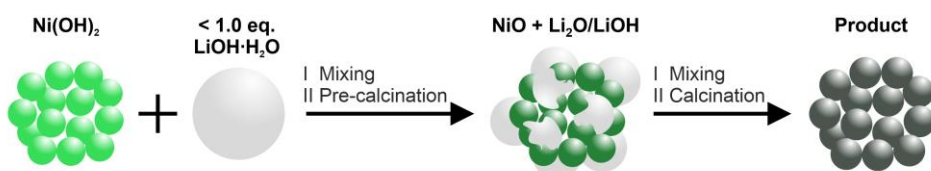


Figure 1. Schematic representations of the state-of-the-art procedure and the residual-free method for the synthesis of Ni-rich CAMs.

The structural parameters of the different materials were determined by Rietveld refinement of XRD data, utilizing a model containing Ni_{Li}^{\bullet} defects [according to $(Li_xNi_{1-x})NiO_2$ or, in short, $Li_xNi_{2-x}O_2$]. From the results in **Table S1**, an inference can be made as to how much lithium should be present in the form of residuals, with full precursor-to-product conversion highlighted by the bold line in **Figure 2a**. Evidently, the samples prepared using the RF method follow this (conversion efficiency) line up

to lithium occupancies of the interlayer spacing of $x \approx 0.98$ in $\text{Li}_x\text{Ni}_{2-x}\text{O}_2$ for RF-Ar and RF-O₂, after which the material quality does not improve further. By contrast, the SoA samples follow a parallel trajectory to the aforementioned line and level off at roughly the same overall quality, although lithium excess in the synthesis is required to achieve this. The difference between nominal and measured stoichiometries can be considered to represent the lithium that is either lost during calcination or deposited onto the surface. The reasonably good agreement in case of the RF samples suggests negligible lithium loss. This was also confirmed by ⁷Li solid-state NMR spectroscopy and SEM measurements (**Figures S2 and S3**). Therefore, increasing the lithium content towards stoichiometric LNO leads to effective lithium-to-nickel ratios close to but below 1:1, beyond which the material quality decreases.

The electrochemical performance of various RF and SoA samples was examined in LIB half-cells in the potential window of 2.9–4.35 vs. Li⁺/Li. The first-cycle specific capacities are plotted against both x and Li/Ni eq. in **Figure 2b** (representative voltage profiles are presented in **Figure S4**). From the distribution of data points, it can be seen that the RF-Ar-0.96 (240 mAh/g) and RF-O₂-0.99 (243 mAh/g) samples delivered the highest q_{dis} . As expected, the capacities decreased with increasing and decreasing lithium content around these substoichiometric LNOs. For lower lithium contents, this is caused by poorer structural quality (higher defect density), whereas for higher lithium-to-nickel ratios, the particle surface becomes increasingly covered by residual lithium, which increases cell resistance. Interestingly, the SoA samples delivered much lower capacities ($q_{\text{dis}} < 230$ mAh/g), even though the $\text{Ni}_{\text{Li}}^{\bullet}$ concentration in SoA-1.01 was similar to that of the best-performing RF samples. To demonstrate that this is related to the presence of residual lithium, SoA-1.01 was washed with water and then re-annealed at 700 °C in an attempt to heal surface damage (SoA-1.01-healed). Despite these post-processing steps, the $\text{Ni}_{\text{Li}}^{\bullet}$ concentration remained virtually unaltered, while the particle surface was freed from residual lithium (**Figures S3**). This is further reflected in the initial q_{dis} (green crosses in **Figure 2b**), which was on par with that achieved with the best-performing RF samples.

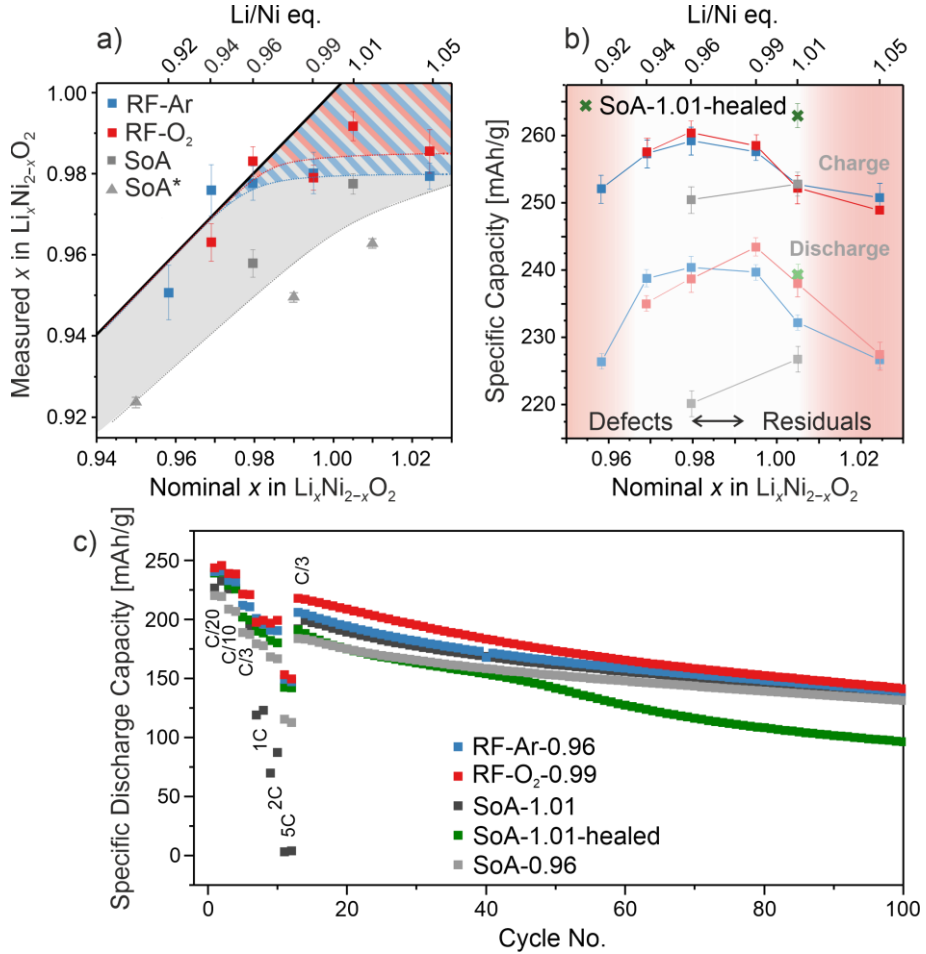


Figure 2. (a) Nominal stoichiometries (synthesis) and measured (XRD) lithium occupancies of the interlayer spacing x in the RF and SoA samples (**Table S1**) calculated by $x = 2 \cdot \text{Li}/\text{Ni}_{\text{eq}}/(1 + \text{Li}/\text{Ni}_{\text{eq}})$. The presence of residual lithium from differences between nominal and measured stoichiometries is highlighted by shaded areas. Ideal behavior is indicated by the bold black line. SoA* results taken from ref. [2]. (b) First-cycle specific capacities at C/20 and (c) rate and long-term cycling performances.

Rate capability tests (**Figure 2c**) also confirmed the poorer performance of those samples where the presence of residual lithium can be assumed such as for SoA-1.01, delivering inferior capacities, especially at rates $\geq 1\text{C}$. Post-treatment mitigates this problem, with SoA-1.01-healed performing similar to RF-Ar-0.96 in the rate capability testing, however at the cost of reduced long-term cycling stability (much stronger fading, especially from the 50th cycle onward). The other RF and SoA samples had a similar long-term performance, albeit with different absolute q_{dis} . The best performance was achieved with RF-O₂-0.99, which is capable of delivering high q_{dis} of 239 mAh/g at C/10 and 221 mAh/g at C/3. These capacities are comparable to the best results reported in the literature for highly engineered CAMs.^[15] Taken together, the results demonstrate that LNO prepared following the RF method outperforms conventionally synthesized (SoA) materials regardless of whether post-treatment steps are involved or not.

To show that the same strategy can also be applied to other Ni-rich CAMs, $\text{LiNi}_x\text{Co}_y\text{Mn}_z\text{O}_2$ (NCM) samples (with Ni:Co:Mn molar ratio of 93.5:4.0:2.5) were synthesized using 0.96 eq. of lithium following the RF-Ar and SoA procedures. Here, 226 and 219 mAh/g (q_{dis}) were achieved, further evidencing a more efficient lithium utilization in case of the RF method.

Overall, the data emphasize the advantages of the substoichiometric synthesis concept over conventional routes. Notably, it allows using less lithium, as well as avoiding tedious post-treatment steps and their detrimental effects, and can be further applied to Ni-rich NCMs.

Conflicts of Interest

The authors declare the following competing interest(s): A patent was filed for some of this work through BASF SE and the Karlsruher Institut für Technologie (KIT).

Supporting Information

Experimental section, results from Rietveld refinements, XRD patterns, ^7Li NMR spectra, SEM images, and voltage profiles.

Acknowledgments

This study was supported by BASF SE. The authors are grateful to the Federal Ministry of Education and Research (Bundesministerium für Bildung und Forschung, BMBF) for funding within the projects SUSTRAB (03XP0415D) and UNIKAM (03XP0484B).

References

- [1] M. Bianchini, M. Roca-Ayats, P. Hartmann, T. Brezesinski, J. Janek, *Angew. Chem. Int. Ed.* **2019**, *58*, 10434.
- [2] D. Goonetilleke, B. Schwarz, H. Li, F. Fauth, E. Suard, S. Mangold, S. Indris, T. Brezesinski, M. Bianchini, D. Weber, *J. Mater. Chem. A* **2023**, *11*, 13468.
- [3] F. Riewald, P. Kurzhals, M. Bianchini, H. Sommer, J. Janek, H. A. Gasteiger, *J. Electrochem. Soc.* **2022**, *169*, 020529.
- [4] P. Kurzhals, F. Riewald, M. Bianchini, H. Sommer, H. A. Gasteiger, J. Janek, P. Kurzhals, M. Bianchini, H. Sommer, J. Janek, H. A. Gasteiger, *J. Electrochem. Soc.* **2021**, *169*, 020529.
- [5] L. Karger, D. Weber, D. Goonetilleke, A. Mazilkin, H. Li, R. Zhang, Y. Ma, S. Indris, A. Kondrakov, J. Janek, T. Brezesinski, *Chem. Mater.* **2023**, *35*, 648.
- [6] L. Karger, S. Korneychuk, W. van den Bergh, S. L. Dreyer, R. Zhang, A. Kondrakov, J. Janek, T. Brezesinski, *Chem. Mater.* **2024**, *36*, 1497.

- [7] Y. Kim, H. Park, J. H. Warner, A. Manthiram, *ACS Energy Lett.* **2021**, *6*, 941.
- [8] S. E. Renfrew, B. D. McCloskey, *J. Am. Chem. Soc.* **2017**, *139*, 17853.
- [9] I. Konuma, N. Ikeda, B. D. L. Campéon, H. Fujimura, J. Kikkawa, H. D. Luong, Y. Tateyama, Y. Ugata, M. Yonemura, T. Ishigaki, T. Aida, N. Yabuuchi, *Energy Storage Mater.* **2024**, *66*, 103200.
- [10] L. Hartmann, D. Pritzl, H. Beyer, H. A. Gasteiger, *J. Electrochem. Soc.* **2021**, *168*, 070507.
- [11] D. Pritzl, T. Teufl, A. T. S. Freiberg, B. Strehle, J. Sicklinger, H. Sommer, P. Hartmann, H. A. Gasteiger, *J. Electrochem. Soc.* **2019**, *166*, A4056.
- [12] X. Li, C. Zhao, J. He, Y. Li, Y. Wang, L. Liu, J. Huang, C. Li, D. Wang, J. Duan, Y. Zhang, *Electrochim. Acta* **2022**, *406*, 139879.
- [13] R. S. Negi, E. Celik, R. Pan, R. Stäglich, J. Senker, M. T. Elm, *ACS Appl. Energy Mater.* **2021**, *4*, 3369.
- [14] P. Kurzhals, F. Riewald, M. Bianchini, S. Ahmed, A. M. Kern, F. Walther, H. Sommer, K. Volz, J. Janek, *J. Electrochem. Soc.* **2022**, *169*, 050526.
- [15] Y. S. G. Park, S. Kim, B. Namkoong, J. Ryu, J. Yoon, N. Park, M. Kim, S. Hand, F. Maglia, *Angew. Chem. Int. Ed.* **2023**, *62*, e202314480.